www.sciencemag.org/cgi/content/full/science.1219631/DC1

Supplementary Materials for

The Tides of Titan

Luciano Iess,* Robert A. Jacobson, Marco Ducci, David J. Stevenson, Jonathan I. Lunine, John W. Armstrong, Sami W. Asmar, Paolo Racioppa, Nicole J. Rappaport, Paolo Tortora

*To whom correspondence should be addressed. E-mail: luciano.iess@uniroma1.it

Published 28 June 2012 on *Science* Express
DOI: 10.1126/science.1219631

This PDF file includes:

Materials and Methods

The sensitivity of k_2 to the interior structure, especially the discrimination between an oceanless Titan and a Titan with an ocean, made its determination one of the main scientific goals of the Cassini mission. However the lack of a scan platform for remote sensing instruments and the use of a fixed high gain antenna required the rotation of the entire spacecraft, forcing the assignment of each flyby to a single instrument and limiting gravity measurements to six passes to date. According to the numbering used by the Cassini project they were T11 (Feb. 27, 2006) T22 (Dec. 28, 2006) T33 (Jun. 29, 2007) T45 (Jul. 29, 2007) T68 (May 20, 2010) and T74 (Feb. 18, 2011) (Table S1). These flybys were distributed along Titan's orbit in order to increase the sensitivity to variations of the gravity field induced by Saturn tidal stresses. Two flybys (T33, T45) occurred near Titan's pericenter, three near the apocenter (T11, T22, T74). T68 was close to quadrature (90° mean anomaly).

Analysis Methods. Two different analyses were carried out in order to increase the confidence in the results. In SOL1 we processed only Doppler data from the six gravity flybys in a multiarc fit. For each flyby we estimated Cassini state vector and the global fit gave us the static gravity field coefficients (including GM) and the real part of k_2. As the orbit of Titan is not perfectly known, the satellite state vector at a reference epoch (18-JAN-2004 00:00:00 UTC) was also estimated. The adjustment of Titan's orbit and mass required also an update of the ephemerides of the major Saturn's satellites in the same iteration. Data from each flyby were iteratively processed using JPL Orbit Determination Program, a proven code used both for spacecraft navigation, planetary geodesy and tests of relativistic gravity *(16,17,18)*.

The second analysis (SOL2) used an extended data set. This included all available radio-metric and optical navigation data from Cassini, data from Voyager and Pioneer and astronomical observations of Saturn and its satellites. All these data were combined in a global solution estimating satellites and planet ephemerides and gravitational parameters of the bodies in the Saturnian system. This procedure, described by Jacobson et al. *(19)*, has been adopted by the Cassini Navigation Team to guide the spacecraft in the Saturn system. Gravity harmonics to degree and order three and the k_2 Love number are estimated from the six gravity flybys, but, differently from SOL1, data from all Titan flybys are used to update Saturn's system ephemerides. The covariance matrix of SOL2 has been de-weighted according to an algorithm specifically developed for planetary gravity analysis. The algorithm accounts for the weakly colored spectrum of interplanetary plasma noise and the corresponding correlation between measurements by suggesting a de-weighting factor for each tracking pass. The use of a degraded weighting matrix results in larger uncertainties (up to a factor of 2) in all estimated parameters.

Estimation of The Love number. Although a recently added capability to JPL's Orbit Determination program (ODP) allows the estimation of a variable gravity field for satellites as well as for planets, SOL1a and SOL1b relied on a separate code for the determination the k_2 Love number and the static gravity field. This procedure entails two main steps. In the first step the partial derivatives of the observable quantities (range rate

in the case at hand) with respect to k_2 are computed. This is accomplished by post-processing intermediate outputs from the ODP. Following *(6)*, the variation of the quadrupole coefficients can be expressed as:

$$\begin{aligned} J_2 &= J_2^{static} - \frac{1}{2} k_2 q_t e \cos M \\ C_{22} &= C_{22}^{static} - \frac{1}{4} k_2 q_t e \cos M \\ S_{22} &= S_{22}^{static} - \frac{1}{6} k_2 q_t e \sin M \end{aligned} \qquad (1)$$

where M is the mean anomaly of Titan with respect to Saturn, e is the eccentricity and

$$q_t = -3 \frac{M_{Saturn}}{M_{Titan}} \left(\frac{R_{Titan}}{a} \right)^3$$

is the tidal parameter, determined by the masses of Saturn and Titan, the radius of Titan and the semimajor axis of the orbit. Its value is -1.19×10^{-4}. Note that the expected peak-to-peak variations of J_2 and C_{22} computed from (1) are

$$\Delta J_2 = J_2(M=\pi) - J_2(M=0) = k_2 q_t e = 1.42 \times 10^{-6} \left(\frac{k_2}{0.4} \right)$$

$$\Delta C_{22} = C_{22}(M=\pi) - C_{22}(M=0) = \frac{1}{2} k_2 q_t e = 0.71 \times 10^{-6} \left(\frac{k_2}{0.4} \right)$$

For k_2=0.4 the variations are respectively 4% and 7% of the static values reported in Table 2 for J_2 and C_{22}. For k_2=0.6 the relative variation increases to 6% and 10.5%. The linear dependence of the harmonic coefficients on the Love number makes the computation of the partial derivatives of the range rate observables z with respect to k_2 particularly simple:

$$\frac{\partial z}{\partial k_2} = \sum_m \frac{\partial z}{\partial C_{2m}} \frac{\partial C_{2m}}{\partial k_2}$$

The first factor in the summation on the right hand side is the partial derivative of the observable with respect to the harmonic coefficients, a quantity that can be directly retrieved from the ODP. The second factor, a function of Titan's mean anomaly at the time of the closest approach, can be easily computed from the model equations (1). We assume that the quadrupole Love number is identical for all degree 2 harmonics. As the dependence of the observables on C_{21} and S_{21} is weak, the actual partial derivative is computed essentially as the sum of the three partials with respect to C_{20} ($-J_2$), C_{22} and S_{22}. The key point is that, in the integration of the variational equations, Titan degree-2 gravity model is represented by the total value of the coefficients for the current arc. We are implicitly making the assumption that the gravity field is constant during the time

span of the flyby, a valid approximation as the flyby duration is much shorter than the Titan orbital period.

Once the partial derivatives with respect to the Love number are computed, they must be included into the information matrix along with partial derivatives for the static component of the gravity field coefficients and the other solve-for parameters. A multiarc approach is used at this stage to obtain a global solution for the gravity field coefficients and the Love number.

The data from all flyby are combined in a multiarc filter that has been validated against the ODP. It computes an iterative, weighted least-square solution, where the information matrix is inverted by means of a batch square-root algorithm to improve the numerical accuracy and stability.

Dynamical Model and Gravity Field. The dynamical model used for trajectory integration in each arc accounts for a variety of forces acting on the spacecraft. The forces of primary interest for this work are the gravitational accelerations due to the Titan GM and the higher degree field. The degree of the field used in the orbital solution was selected as the lowest capable of fitting the data without producing signatures at closest approach. A 3x3 field (see Table 1) is adequate and the resulting post-fit residuals show no signatures and a RMS value compatible with the expected noise level for each flyby (Fig. S1). We have also produced a 4x4 field (Table S2) with the goal of assessing the stability of the estimated parameters (in particular k_2) to changes in the solution rank. The geoid obtained from this solution is shown in Fig. S3.

Titan pole direction (see Table S3) was set according to the determination obtained by SAR landmark tracking *(20)*. Other forces include the point mass accelerations due to all the other bodies of the solar system (mainly Saturn and its satellites, the Sun and Jupiter), solar pressure and thermal thrust from Cassini's RTG (Radio-isotope Thermoelectric Generators). The acceleration from the three RTG has been very precisely determined from years of tracking data. Its current uncertainty has been considered in the generation of the covariance matrices. Titan atmospheric drag is neglected except for flybys whose altitude at closest approach is lower than 1350 km. Thus no drag acceleration is accounted for in all flybys with the exception of T22. The ODP uses a relativistic formulation of solar system dynamics to the order $1/c^2$. Higher order approximations are used in the solution of the light time problem. Whenever available, path delay variations due to tropospheric water vapor were compensated using measurements from two microwave radiometers located near the tracking antennas in Spain and California.

The reference solution for Titan's static gravity uses a full 3x3 harmonic expansion, for a total of 12 coefficients (J_2, C_{21}, S_{21}, C_{22}, S_{22}, J_3, C_{31}, S_{31}, C_{32}, S_{32}, C_{33}, S_{33}). Its stability, both for the static and variable components, was tested by estimating also a 4x4 gravity model (therefore adding 9 parameters to the solution). Although a priori uncertainties were used for the gravity coefficients, the constraints were on average two orders of magnitude larger than the formal uncertainties at the end of the estimation process. Increasing by one order of magnitude the a priori uncertainties of all estimated parameters did not change the solution in any statistically significant way. Tighter constraints were used only for C_{21} and S_{21}, because the obliquity of Titan is well determined by SAR data. The a priori uncertainties were set to allow an obliquity

variation of 1° (which is more than three times the estimated value *(20)*). Adopting the IAU rotational model did not produce any significant effect on the solution.

At the first iteration, nominal values of the largest gravity coefficients (J_2 and C_{22}) were set according to a previous determination *(1)*, namely $J_2 = 3.33 \times 10^{-5}$ and $C_{22} = 1.0 \times 10^{-5}$. All the other coefficients were initialized to zero. The hydrostatic constraint (J_2/C_{22}=10/3) was never used. However, all the solutions yield a J_2/C_{22} ratio of 3.320±0.034 (SOL1a) and 3.353±0.039 (SOL2), fully compatible with hydrostatic equilibrium. The solution also includes the estimate of Cassini's state vector (position and velocity) for each arc. Covergence is obtained within three iterations, although five iterations are routinely performed to verify the stability of the solution.

Data weighting is performed on a pass-by-pass basis. In SOL1 weights are assigned as the inverse of the variance of the post-fit residuals for that pass, iteratively until convergence. The RMS value of the residuals of the fitted arc is reported in Table S1. The correctness of the weight assignment is checked against the post-fit sum of the squared, weighted residuals (SOS), which must be close to the number of observations used in the fit. In SOL2, correlations due to the dominant noise source (interplanetary plasma) are accounted for in a de-weighting procedure described in the Supplementary Online Material of *(1)*.

In the previous paper *(1)* variable gravity was not accounted for in the fit. This approach was justified by the even distribution of the four flybys between pericenter and apocenter of Titan's orbit, a circumstance that effectively averaged out the effects of eccentricity tides in the combined solution. However, this qualitative argument did not guarantee that the suboptimal dynamical model would not result in a bias of some components of the solution (e.g. the spacecraft state vector). Indeed, although the static gravity field obtained in *(1)* is confirmed, the absence of eccentricity tides in the previous analysis was a significant limitation. In that previous work the effect of variable gravity was absorbed by other parameters. In the current work static gravity is retrieved if $k_2 = 0$. If k_2 is forced to zero (therefore decreasing the rank of the solution from 56 to 55), the RMS value of the residuals near closest approach increases for all passes (see table S4). The increase is particularly significant for the best passes (T11, T22 and T33), where the degradation is respectively 11%, 20% and 8%. Applying additional constraints always results in residuals with signatures (very large in case 2 and 3). All constraints result in a bias and aliasing of the estimated parameters. Although the RMS values support our approach, the strong geophysical arguments militating in favor of a significant time-dependent gravity (driven by the large eccentricity) make the dynamical model adopted in the current analysis more appropriate and superior. While excluding k_2 from the solution could certainly bias some parameters, its inclusion does not harm in any way: the only effect of the additional parameter (k_2) would be an increase in the uncertainties of the gravity coefficients, an effect that did not occur because of the additional information provided by the new flybys (T68 and T74).

Fig. S1.

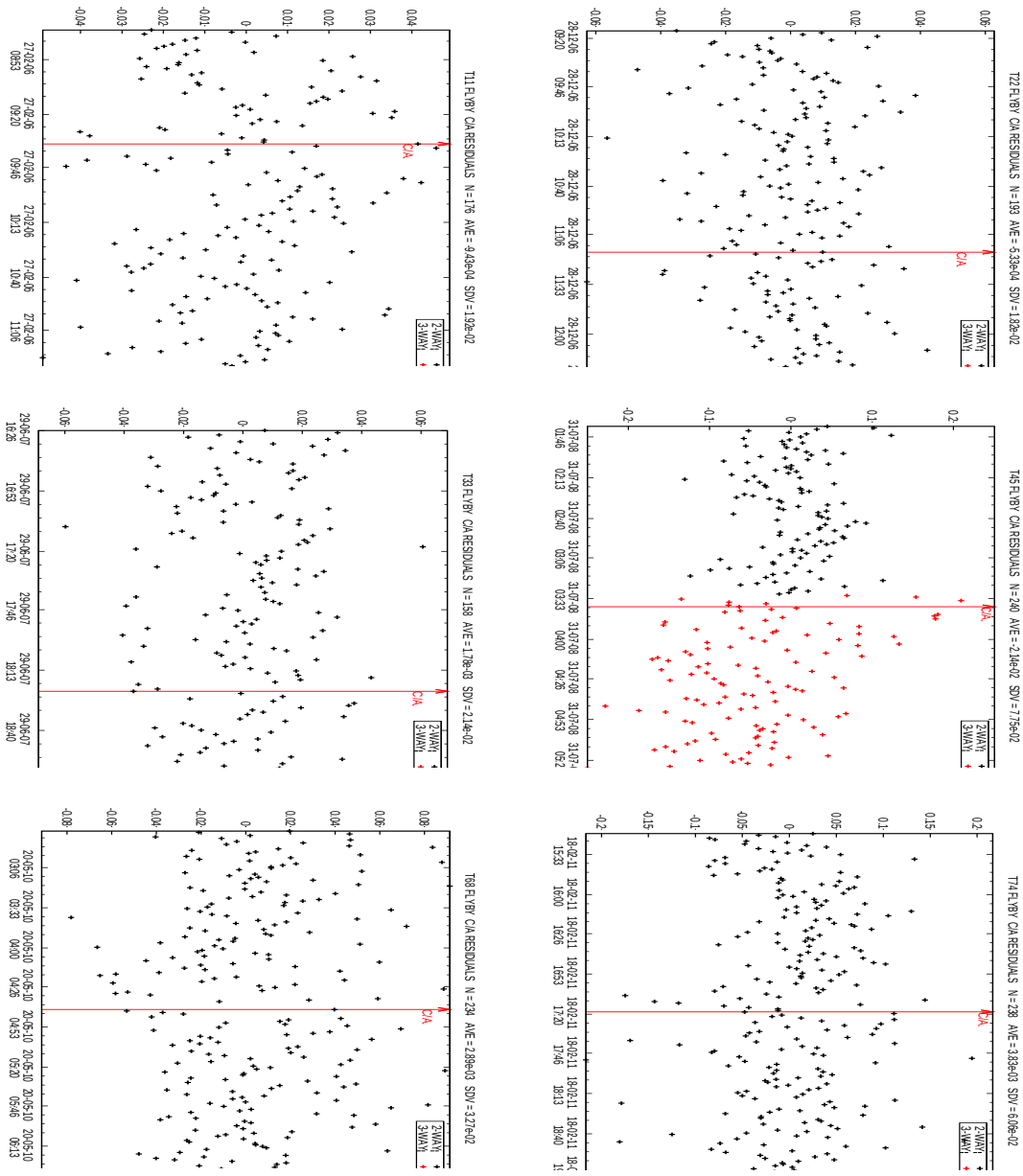

Fig. S1: Doppler residuals (in mm/s) around closest approach for all six flybys (SOL1a). Time span is about three hours.

Fig. S2

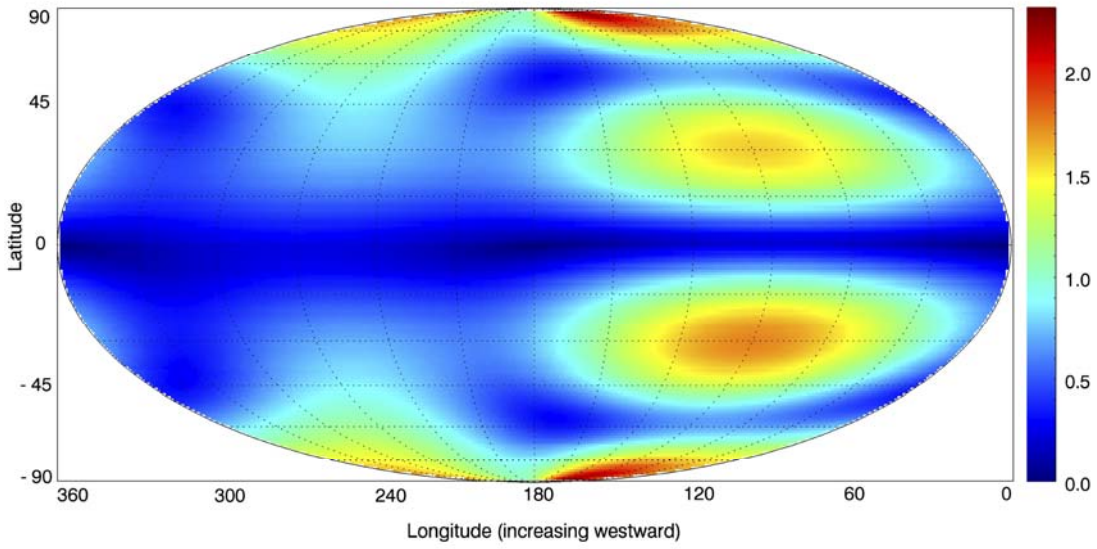

Fig. S2: Estimated uncertainties in the 3x3 geoid heights, derived from the covariance matrix of the gravity solution SOL1a, and referred to the reference ellipsoid defined by GM, J2, C22 and ω.

Fig. S3

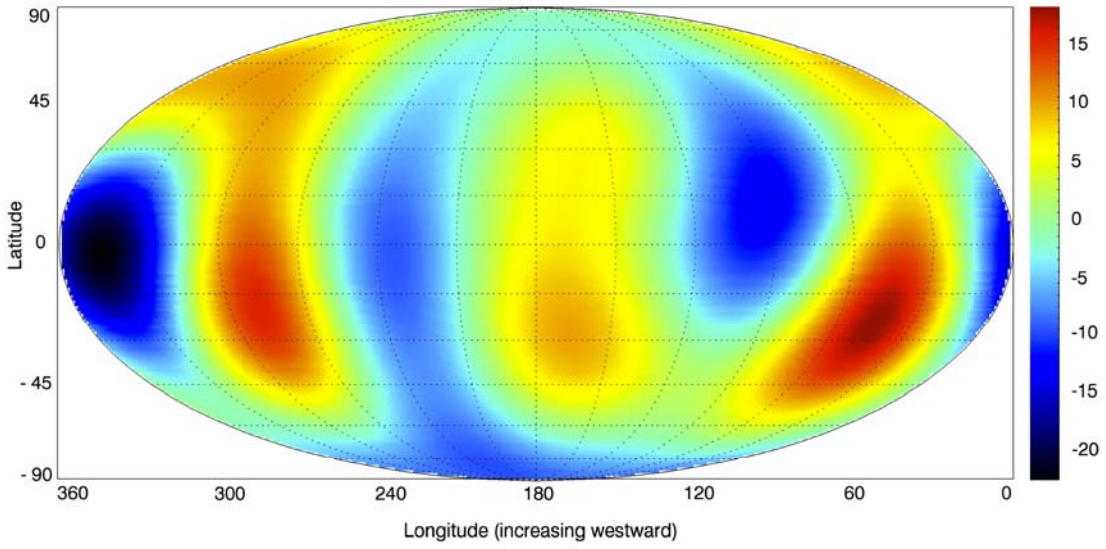

Fig. S3: Geoid heights for the 4x4 gravity field (SOL1b, Table S3), referred to the reference ellipsoid defined by GM, J2, C22 and ω.

Table S1.

Table S1: Geometric and orbital parameters of the six flybys used in the determination of k_2 and the static gravity field. NOISE is the RMS value of post-fit residuals in SOL1a for the entire observed arc (about +/-24 hours). SEP is the sun-earth-probe angle. Noise due to interplanetary plasma turbulence is minimum near solar oppositions (SEP = 180 deg).

	T11	T22	T33	T45	T68	T74
DATE	27-FEB-2006 08:25:18 ET	28-DEC-2006 10:06:27 ET	29-JUN-2007 17:00:51 ET	31-JUL-2008 02:14:16 ET	20-MAY-2010 03:25:26 ET	18-FEB-2011 16:05:17 ET
MEAN ANOM.	172.7°	197.3°	15.1°	346.2°	81.8°	15.9°
SEP	147.0°	131.9°	44.6°	29.4°	118.8°	133.0°
ALTITUDE (km)	1812	1297	1933	1614	1399	3652
LATITUDE	-0.2°	40.6°	8.4°	-43.5°	-49.0°	0.7°
LONGITUDE	250.6°	0.0°	63.1°	162.7°	241.5°	113.4°
INCLINATION	179.7°	67.3°	8.4°	122.3°	130.9°	179.3°
N. OF POINTS	1134	1292	1435	1303	1911	1627
NOISE (mm/s)	0.021	0.023	0.028	0.074	0.037	0.071

Table S2.

Table S2: Rotation model adopted for the gravity solutions (SOL1a, SOL1b, SOL2). *T* is given in Julian centuries (of 36525 days) past J2000, *d* are days past J2000.

	Rotation model
α_0	38°.242151-0.04229*T*
δ_0	83°.768864-0.00444*T*
W_0	189°.861726+22.5769791934*d*

Table S3.

Table S3: Coefficients of the un-normalized spherical harmonics for the 4x4 gravity field (SOL1b). See Fig. S3 for the associated geoid heights.

	SOL1b		
	VALUE	±1σ	($\times 10^{+06}$)
J2	34.227	±	0.477
C21	0.125	±	0.111
S21	0.816	±	0.351
C22	10.263	±	0.069
S22	0.111	±	0.055
J3	-1.635	±	0.838
C31	0.681	±	0.207
S31	-0.073	±	0.475
C32	0.150	±	0.125
S32	0.104	±	0.114
C33	-0.221	±	0.016
S33	-0.232	±	0.016
J4	2.043	±	0.759
C41	0.175	±	0.203
S41	0.033	±	0.250
C42	0.059	±	0.080
S42	0.093	±	0.058
C43	0.026	±	0.015
S43	0.008	±	0.020
C44	-0.007	±	0.002
S44	-0.014	±	0.002

Table S4

Table S4: RMS value of the residuals (in mm/s x 100) for a short arc spanning +/-10 min. from closest approach (covering most of the quadrupole signal), when different constraints are applied to the solution, namely:

- Case 1: Estimate of 3x3 static field (k_2=0), Titan and Cassini state vectors.
- Case 2: Estimate of 3x3 static field (k_2=0). Titan and Cassini SV constrained to the values of SOL1.a
- Case 3: Estimate of 3x3 static field (k_2=0) and Titan SV. Cassini SV constrained to the values of SOL1.a
- Case 4: Estimate of 3x3 static field (k_2=0) and Cassini SV. Titan SV constrained to the values of SOL1.a

+/-10 min	**Sol1.a**	**Case 1**	**Case 2**	**Case 3**	**Case 4**
T11	2.36	2.61	6.23	5.47	2.81
T22	1.67	2.00	12.1	11.7	2.70
T33	2.38	2.57	11.5	6.86	2.45
T45	10.6	11.1	13.5	30.9	17.9
T68	3.53	3.54	19.2	12.0	7.66
T74	7.52	7.78	9.87	17.8	8.11

References and Notes

1. L. Iess *et al*., Gravity field, shape, and moment of inertia of Titan. *Science* **327**, 1367 (2010). doi:10.1126/science.1182583 Medline

2. N. Rappaport *et al*., Doppler measurements of the quadrupole moments of Titan. *Icarus* **126**, 313 (1997). doi:10.1006/icar.1996.5661

3. See the supplementary materials for additional discussion.

4. Thanks to the use of X- and Ka-band (8.4 and 32.5 GHz) frequencies and state-of-the-art instrumentation, range-rate accuracies were in the range from 2×10^{-5} to 9×10^{-5} m/s at integration times of 60 s, depending on the solar elongation angle. The dependence is due to interplanetary plasma noise, which dominates the Doppler error budget (*15*).

5. A determination of the complex Love number yields a value for imaginary (Im)(k_2) compatible with zero at the 1σ level. Because the flybys and their geometry were selected to maximize the sensitivity to the real part of k_2, the estimate of Im(k_2) is less stable than for the real counterpart.

6. N. Rappaport *et al*., Can Cassini detect a subsurface ocean in Titan from gravity measurements? *Icarus* **194**, 711 (2008). doi:10.1016/j.icarus.2007.11.024

7. G. H. Darwin, On the bodily tides of viscous and semi-elastic spheroids, and on the ocean tides upon a yielding nucleus. *Philos. Trans. R. Soc. Lond.* **170**, 1 (1879). doi:10.1098/rstl.1879.0061

8. D. L. Goldsby, D. L. Kohlstedt, Superplastic deformation of ice: Experimental observations. *J. Geophys. Res. Solid Earth* **106**, 11017 (2001). doi:10.1029/2000JB900336

9. J. C. Castillo-Rogez, J. I. Lunine, Evolution of Titan's rocky core constrained by Cassini observations. *Geophys. Res. Lett.* **37**, L20205 (2010). doi:10.1029/2010GL044398

10. G. Tobie, O. Grasset, J. I. Lunine, A. Mocquet, C. Sotin, Titan's internal structure inferred from a coupled thermal-orbital model. *Icarus* **175**, 496 (2005). doi:10.1016/j.icarus.2004.12.007

11. A. D. Fortes, P. Grindrod, S. Trickett, L. Vocadlo, Ammonium sulfate on Titan: Possible origin and role in cryovolcanism. *Icarus* **188**, 139 (2007). doi:10.1016/j.icarus.2006.11.002

12. F. Paganelli *et al*., Titan's surface from the Cassini RADAR radiometry data during SAR mode. *Planet. Space Sci.* **56**, 100 (2008). doi:10.1016/j.pss.2007.03.015

13. F. Sohl, Planetary science. Revealing Titan's interior. *Science* **327**, 1338 (2010). doi:10.1126/science.1186255 Medline

14. C. Béghin, C. Sotin, M. Hamelin, Titan's native ocean revealed beneath some 45km of ice by a Schumann-like resonance. *C. R. Geosci.* **342**, 425 (2010). doi:10.1016/j.crte.2010.03.003

15. S. W. Asmar *et al*., Spacecraft Doppler tracking: Noise budget and accuracy achievable in precision radio science observations. *Radio Sci.* **40**, RS2001 (2005). doi:10.1029/2004RS003101

16. F. Pelletier *et al*., paper AAS 12-209 presented at the 22nd American Astronomical Society/American Institute of Aeronautics and Astronautics Space Flight Mechanics Meeting, Charleston, SC, 29 January 2012.

17. A. S. Konopliv, C. F. Yoder, E. M. Standish, D.-N. Yuan, W. L. Sjogren, A global solution for the Mars static and seasonal gravity, Mars orientation, Phobos and Deimos masses, and Mars ephemeris. *Icarus* **182**, 23 (2006). doi:10.1016/j.icarus.2005.12.025

18. B. Bertotti, L. Iess, P. Tortora, A test of general relativity using radio links with the Cassini spacecraft. *Nature* **425**, 374 (2003). doi:10.1038/nature01997 Medline

19. R. A. Jacobson *et al*., The gravity field of the saturnian system from satellite observations and spacecraft tracking data. *Astron. J.* **132**, 2520 (2006). doi:10.1086/508812

20. P. Persi Del Marmo *et al*., *Eos Trans. AGU* **88**, 21D (2007).